Low-Frequency Signals in Midtropospheric Submonthly Temperature Variance

HAIG ISKENDERIAN AND RICHARD D. ROSEN

Atmospheric and Environmental Research, Inc., Cambridge, Massachusetts

(Manuscript received 26 April 1999, in final form 22 September 1999)

ABSTRACT

Low-frequency signals in the daily variability of temperature in the midtroposphere are investigated, thereby complementing published studies of changes in day-to-day temperature variability and in extreme weather events at the surface. The results are based upon approximately four decades of upper-air data from radiosondes and the National Centers for Environmental Prediction–National Center for Atmospheric Research (NCEP–NCAR) reanalyses. The annual mean field of 500-hPa submonthly temperature variance, var(T), is oriented zonally across most of the globe, with maxima in the midlatitudes over the major landmasses of North America and Asia and over the oceans of the Southern Hemisphere. Seasonally, var(T) shifts equatorward from the warm to cool season in both hemispheres. Therefore, var(T) reflects day-to-day changes in temperature about the jet stream associated with baroclinic synoptic-scale systems.

Year-to-year changes in var(T) over the Northern Hemisphere are greatest over the major landmasses of North America, northern Europe, and Asia. There is also evidence of an influence of ENSO upon the interannual variability of var(T) over the northern portion of North America during winter, where there is a westward displaced maximum in cold events relative to warm events. Trend analysis over the Northern Hemisphere shows that there has been a significant increase in submonthly temperature variance over the northeastern portion of North America, the North Atlantic, and Scandinavia, representing as much as 30% of the climatological values of var(T) in these regions. These regional trends are most apparent during the Northern Hemisphere winter and spring seasons.

The zonally averaged var(T) has generally decreased over polar latitudes and increased over the midlatitudes of the Northern Hemisphere, although there are considerable differences from season to season. Averaged over the entire Northern Hemisphere, var(T) exhibits a slight upward trend since the late 1950s in the NCEP–NCAR reanalysis, although this trend is significant in the spring season only. The robustness of this springtime trend, however, is in doubt, because the trend found from a radiosonde-only dataset is negative. For the conterminous United States, the two datasets do agree by showing mostly small positive trends in most seasons. These positive trends, however, are not statistically significant, and therefore the authors cannot state with confidence that there has been a change in synoptic-scale temperature variance in the midtroposphere over the United States since 1958.

1. Introduction

Increasing scientific attention is turning to the identification of interdecadal variability in the climate of the recent past. Studies of observed low-frequency variations in climate during the last hundred years or so are becoming more numerous as series of historical data lengthen, while simulations of such variations by general circulation models have been made feasible by advances in computer resources (see, e.g., Mann and Park 1996, and references therein). Whereas a broad spectrum of climate variability has been revealed in both kinds of investigations, the results are often inconsistent between models and observations or from model to model (Kim et al. 1996), requiring that the subject receive further attention. Changes in the frequency or intensity of extreme weather events deserve particular focus because these factors may be of greater relevance to the biosphere and society than changes in the mean state of the climate system per se. The likelihood of extreme events appears in turn to be at least as sensitive to changes in the variability of climate as to changes in its average (Katz and Brown 1992; Tarleton and Katz 1995; Wagner 1996; Karl and Knight 1997).

The notion that climate may have become more ‘‘variable’’ in recent times is by no means new. More than twenty years ago, for example, the scientific community was concerned that ‘‘since the 1940’s and 1950’s . . . the atmospheric circulation in the Northern Hemisphere appears to have shifted in a manner suggestive of an increasing amplitude of the planetary waves and of greater extremes of weather conditions in many areas of the world’’ (GARP 1975, p. 16). Recent events in the form of heat waves, droughts, floods, and hurricanes have led to a resurgence of interest in the societal impacts of climate variability (Kunkel et al. 1999) and to renewed efforts to characterize the frequency of extreme

Corresponding author address: Dr. Richard D. Rosen, Atmospheric and Environmental Research, Inc., 840 Memorial Dr., Cambridge, MA 02139.
E-mail: rdrosen@aer.com

events. In the case of tropical cyclone frequency, for example, observational studies searching for trends have been undertaken by Landsea et al. (1996), Chan and Shi (1996), Bove et al. (1998), and Henderson-Sellers et al. (1998), and modeling studies aimed at predicting changes in hurricane frequency under doubled CO_2 conditions have been undertaken by Bengtsson et al. (1996) and others.

On the scale of the conterminous United States, attempts to detect a trend toward more anomalous behavior in the climate system have led to the development of a Climate Extremes Index (CEI) by Karl et al. (1995a,b). The CEI involves annual measures of the percent of the United States with much above or much below temperature or precipitation during the period since 1910; the authors find that this index increased abruptly during the 1970s and has remained elevated since. In a more ambitious effort, Karl et al. (1995c) consider trends in high-frequency climate variability at hundreds of surface-based stations in Asia and Australia, in addition to stations in the United States. Nicholls et al. (1996) caution, however, that although changes in climate variability may be demonstrated on regional scales, evidence for an overall global trend in climate variability during this century is lacking.

Model predictions of changes in variability in a warmer climate are neither plentiful nor definitive (Barron 1995). Rind et al. (1989) find that the daily variability in surface temperature over the United States does not change significantly in their simulations of warmer climates, although there is a tendency for decreased variability. They suggest that this generally null result may represent the competing effects in their model of a weaker latitudinal temperature gradient at the surface (and hence weaker synoptic-scale waves) in an enhanced-CO_2 atmosphere and a stronger gradient aloft. In a doubled-CO_2 experiment with another global climate model, Lambert (1995) finds that there is a significant reduction in the total number of wintertime cyclones in both hemispheres, but the frequency of intense cyclones increases, perhaps because of the higher levels of humidity, and hence latent heat, in the warmer climate (Held 1993). Observations suggest that the number of extratropical winter cyclones over the North Pacific and North Atlantic has increased noticeably since 1970 (Lambert 1996), although over the northeast Atlantic and North Sea, at least, the intensities of present-day storms may be comparable to those at the beginning of the century (The WASA Group 1998).

A common thread among most studies of climate variability thus far is their focus on behavior at the surface, although several modeling efforts have attempted to relate increases in greenhouse forcing to changes in upper-air high-frequency transient activity. Bates and Meehl (1986), Branscome and Gutowski (1992), Boer (1995), and Zhang and Wang (1997) all obtain decreases in assorted measures of upper-air transient activity in model runs with increased CO_2. On the other hand, Gutowski et al. (1995) find that opposite results can be obtained depending on the model used, echoing a similar warning by Rind et al. (1989). Observed changes in upper-air climate variability against which to test model experiments are not plentiful, a situation that we hope to partially ameliorate here.

Linkages between changes in surface and upper-air variability undoubtedly exist, of course. Karl et al. (1995b), for example, relate the origin of the abrupt change in the behavior of their CEI in the 1970s to major circulation changes that occurred over the Pacific Ocean and North America then (Trenberth and Hurrell 1994; Mantua et al. 1997). On the other hand, there is also evidence that decadal and other low-frequency variations in the troposphere may be decoupled from such signals near the surface: witness, for example, the apparently different trends in global-mean temperature reported for the lower troposphere (Christy et al. 1995; Basist and Chelliah 1997; Parker et al. 1997) and for the surface for the same epoch (Hurrell and Trenberth 1996; but see Prabhakara et al. 1998; Wentz and Schabel 1998; Santer et al. 1999). It is important, therefore, to document trends in upper-air variability, as we attempt here, both for their own sake and as a prelude to diagnosing the dynamics associated with surface manifestations of climate change.

Those studies that have dealt with climate trends in the upper air have tended to focus on trends in the mean quantities rather than on trends in their variability. Oort and Liu (1993), for example, calculated trends in monthly mean temperatures at individual upper-air levels across the globe using analyses based on the Geophysical Fluid Dynamics Laboratory radiosonde dataset for 1958–89. As early as Boer and Higuchi (1980), however, the importance of identifying trends not only in the means of upper-air quantities but also in their variance has been recognized. Boer and Higuchi applied variance analysis to zonal-mean features of the 1000–500-hPa thickness field north of 25°N based on British Meteorological Office geopotential height analyses for 1949–75. When the data are stratified seasonally (Boer and Higuchi 1981), significant trends in the hemispheric-mean submonthly variance of the thickness field are found in spring and, especially, summer. Considering the restriction of the Boer and Higuchi analyses to zonal-mean variance prior to 1975, attempts to reconsider the regional and hemispheric low-frequency behavior of upper-air variability seem overdue. The emergence of additional datasets, described below, provides an important opportunity to extend those results and is a major incentive for the current study.

2. Datasets

This study reports on the secular trends in midtroposphere temperature variance. Two datasets of sufficient length to undertake this analysis are described below. We have chosen the 500-hPa level for our analysis because this level lies largely within the free troposphere at all latitudes for all seasons, and the patterns of var(T) at this level are representative of the troposphere as a whole (Peixoto and Oort 1992).

a. Oort data and statistics

The ''Oort'' dataset, based solely upon radiosonde observations from approximately 800 regularly reporting stations mainly on land across the globe, provides monthly mean values of var(T) at a number of upper-air levels on a 2.5° lat × 5° long grid for the 31-yr period of December 1958–November 1989. These monthly mean fields are derived from 0000 and 1200 UTC data, except during the 5-yr period of May 1958–April 1963 when the fields are based on 0000 UTC data only. As described by Oort and Liu (1993), a cutoff criterion was applied to ensure that only stations reporting a certain minimum number of days per month were used in creating the analyses. This criterion changed with time, and other inhomogeneities exist in the Oort data and statistics, but Oort and Liu demonstrate that these seem not to seriously affect their estimates of trends in upper-air mean temperature. Results regarding the general circulation based on the Oort data are prominent in the literature, and the strengths and weaknesses of these data are, therefore, well known. Encouragingly, results for tropospheric temperature trends derived from this dataset generally agree with those obtained from the 63-station dataset of Angell (1990) and from satellite microwave data for periods of overlapping measurements (Oort and Liu 1993). Parker et al. (1997) have reexamined upper-air temperature trends with monthly radiosonde data that are adjusted for instrument-related discontinuities; their initial results are also broadly consistent with those of Oort and Liu.

b. NCEP–NCAR reanalysis

Recognizing that operational gridded analyses are not well suited for analyzing low-frequency climate variations because the components of the analysis systems are continually being upgraded or changed in some way, reanalysis projects have been undertaken at the National Centers for Environmental Prediction with the National Center for Atmospheric Research (NCEP–NCAR) and elsewhere in which daily retrospective analyses of the atmosphere are produced with a fixed, state-of-the-art data assimilation system. A distinguishing feature of the NCEP–NCAR reanalysis project (Kalnay et al. 1996) is its having generated multidecadal analyses, thereby creating an upper-air time series lengthy enough for climate variability studies. An important advantage of the NCEP–NCAR reanalyses over the Oort dataset is that information from a variety of platforms is used; however, prior to the 1970s these data mainly consist of radiosonde measurements. While the inclusion of satellite data may introduce bias into the reanalysis temperature values (Santer et al. 1999), inspection of our time series of var(T) over land and ocean regions shows little evidence of a discontinuity. For this study, we have chosen to use the 500-hPa temperature analyses available four times daily on a 2.5° × 2.5° global grid for the 38-yr period of December 1958–November 1996. We averaged the four-times daily temperature fields into daily means, and submonthly temperature variances at each grid point were computed from these daily means according to the procedure described below.

3. Method

The upper-air datasets described above allow us to consider behavior of temperature variance over a multidecadal period. Denoting temperature at the 500-hPa level by the symbol T, then because T is a function of latitude (ϕ), longitude (λ), and time (t), the following definitions for the temporal variance of T at a point in space may be given:

$$\overline{T'^2}(\phi, \lambda) = \mathrm{var}(T) = \overline{(T - \overline{T})^2}, \qquad (1)$$

where

$$\overline{T}(\phi, \lambda) = \frac{1}{\tau} \int T\, dt, \qquad (2)$$

and T is sampled on a daily mean basis and the time averaging is taken over a month (i.e., $\tau = 1$ month). Hence, var(T) measures the day-to-day variability of 500-hPa temperature within a month. We first computed var(T) for each month and then averaged monthly values to create seasonal means for four seasons: December–February (DJF); March–May (MAM); June–August (JJA); and September–November (SON).

As a measure of year-to-year variability, we computed the interannual standard deviation in var(T) for the four canonical seasons based on the 31 (Oort) or 38 (NCEP–NCAR) yr of data. Linear trends in var(T) are calculated as the slope of the linear regression line fit to the time series of var(T) at each grid point. As in Ross and Elliott (1996), we base the significance of the linear trend upon the Spearman rank correlation coefficient (Wilks 1995) r_s given by

$$r_s = 1 - \frac{6 \sum_{i=1}^{n} D_i^2}{n(n^2 - 1)}, \qquad (3)$$

where D_i is the difference in ranks between the ith pair of data values and n is the number of elements in the time series. A Student's t statistic is computed according to

$$t = r_s \sqrt{\frac{n - 2}{1 - r_s^2}}. \qquad (4)$$

As in Venne and Dartt (1990), we computed 1-yr lag autocorrelation coefficients at each grid point and then examined these over the Northern Hemisphere to assess the degrees of freedom in the seasonal-mean data. In the case of the NCEP–NCAR reanalysis, for example, we determined that little autocorrelation exists, so that the level of confidence in the linear trend of var(T) could be assessed relative to a two-tailed Student's t test assuming 36 (i.e., $n - 2$) degrees of freedom.

4. Results

We present the ''climatology'' of the 500-hPa var(T) for the entire globe in section 4a. Because the sparsity of observations in the Southern Hemisphere limits confidence in results there, maps of year-to-year changes in var(T) as measured by the interannual standard deviation of var(T) are presented for the Northern Hemisphere only, in section 4b. Secular trends in var(T), both regionally and for the Northern Hemisphere as a whole, are presented in section 4c.

a. The climatology of 500-hPa temperature variance

The seasonal-mean var(T) during the four seasons for 38 yr (December 1958–November 1996) of NCEP–NCAR reanalysis data is shown in Fig. 1. In general, the largest values of var(T) occur in the cool season of the respective hemisphere, and var(T) is larger in the Northern than in the Southern Hemisphere. In the Northern Hemisphere, the maximum values tend to lie over the land, whereas in the Southern Hemisphere, maximum values occur over the data-sparse oceans. Further, there is an equatorward shift in the maximum values from warm to cool seasons. The equatorward shift, the seasonal dependence, and the zonal orientation of var(T) are consistent with var(T) being associated with submonthly temperature fluctuations in the midlatitude westerlies brought about by synoptic-scale systems.

Figure 2 shows the Northern Hemisphere time-mean 500-hPa var(T) from the Oort and NCEP–NCAR datasets for the 31-yr period of overlap (December 1958–November 1989). The Oort data also show the zonal orientation and the large values of var(T) over the landmasses of North America and Asia. Even though the locations of these features are consistent between the two datasets, the maximum values of var(T) in the Oort data tend to be about 20% larger than in the NCEP–NCAR data.

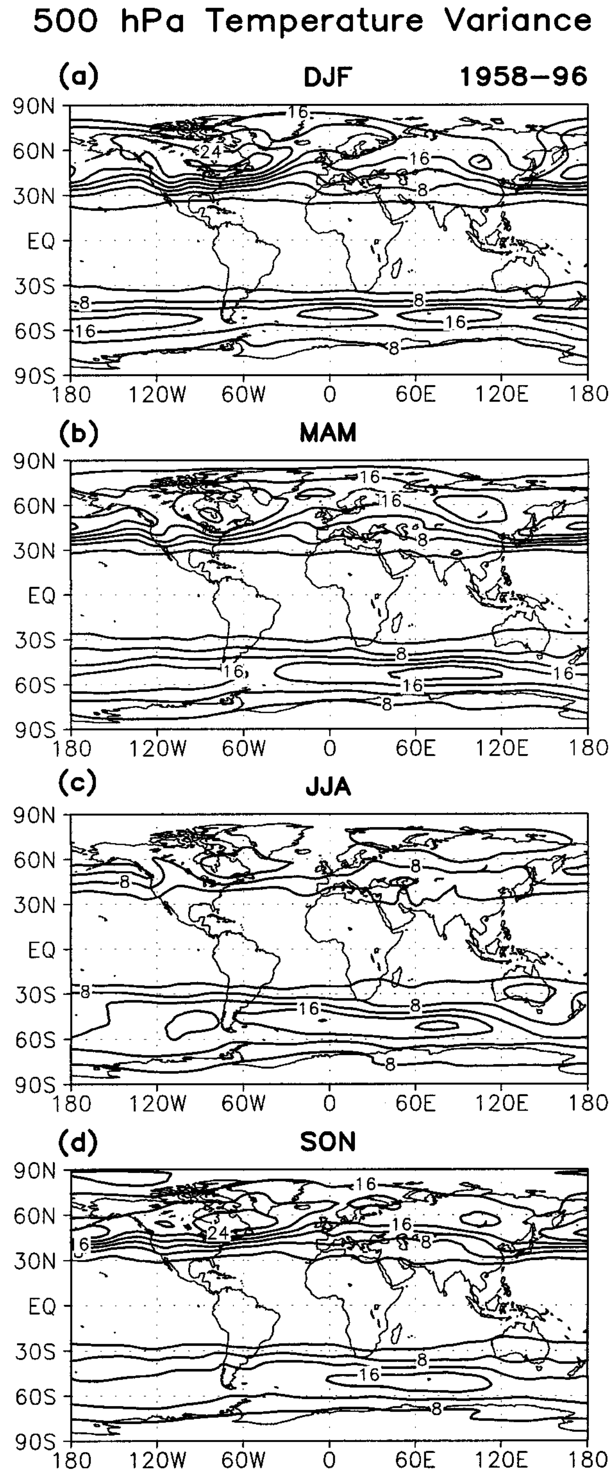

FIG. 1. The 500-hPa temperature variance from the NCEP–NCAR reanalysis for the 38-yr period of Dec 1958–Nov 1996 for (a) DJF, (b) MAM, (c) JJA, and (d) SON. Values every 4°C² are contoured.

b. The interannual variability in 500-hPa temperature variance

The year-to-year variability of Northern Hemisphere winter temperature variance is represented by the interannual standard deviation of DJF var(T) from the NCEP–NCAR dataset (Fig. 3). The linear trend, discussed in section 4c below, has been removed from the fields prior to this calculation. The interannual standard

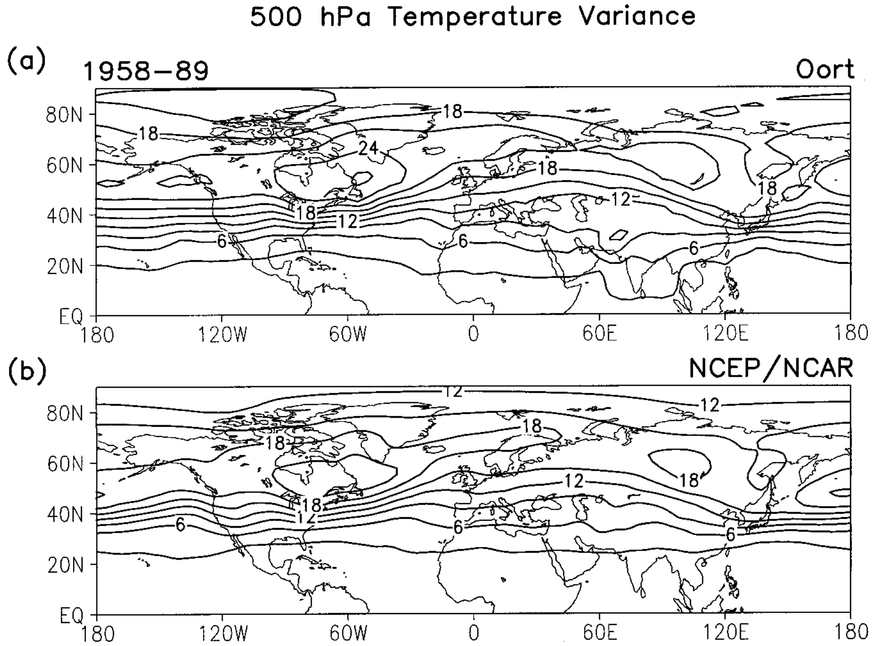

FIG. 2. The 500-hPa temperature variance for the 31-yr period of Dec 1958–Nov 1989 for (a) the Oort radiosonde dataset and (b) the NCEP–NCAR reanalysis. Values every 3°C² are contoured.

deviation of var(T) generally increases poleward from the Tropics, reaching maxima in the northern portions of the continents of North America, Europe, and Asia. These maxima reach values of 6°–8°C², or about 30% of the seasonal-mean DJF values in these areas (Fig. 1a). Interestingly, these centers of large interannual variability in var(T) are over land. This is also true of the interannual standard deviation of monthly mean temperature in the lower troposphere (Gutzler et al. 1988) and at the surface (Barnett 1978), and is in contrast to geopotential height whose centers of maximum interannual variance tend to lie over the oceans (Blackmon et al. 1979).

To determine whether the variability in the centers in Fig. 3 is interrelated, we correlated the time series of var(T) at points in the center of the three maxima with all other points in the Northern Hemisphere and found little evidence for teleconnections. For a separate check on the presence of teleconnection patterns, we computed empirical orthogonal functions (EOFs, not shown) from the detrended time series of DJF var(T) on an equal area grid to determine if the interannual variance of var(T) exhibited any spatially coherent structure in the Northern Hemisphere. The first mode, explaining only 16% of the total variance in the fields, showed simply a localized maximum over the northern portion of North America.

Further examination of the time series of this first EOF indicates different polarities of the signal between warm and cold events of the El Niño–Southern Oscil-

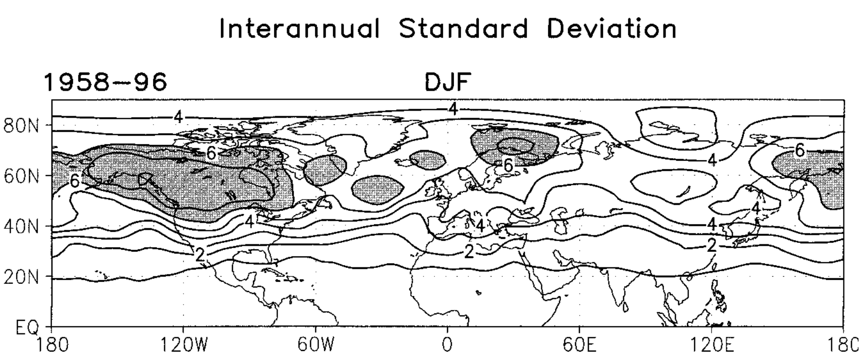

FIG. 3. Interannual standard deviation of DJF 500-hPa temperature variance from the NCEP–NCAR reanalysis for the 38-yr period of Dec 1958–Nov 1996. Values every 1°C² are contoured, and values greater than 6°C² are shaded.

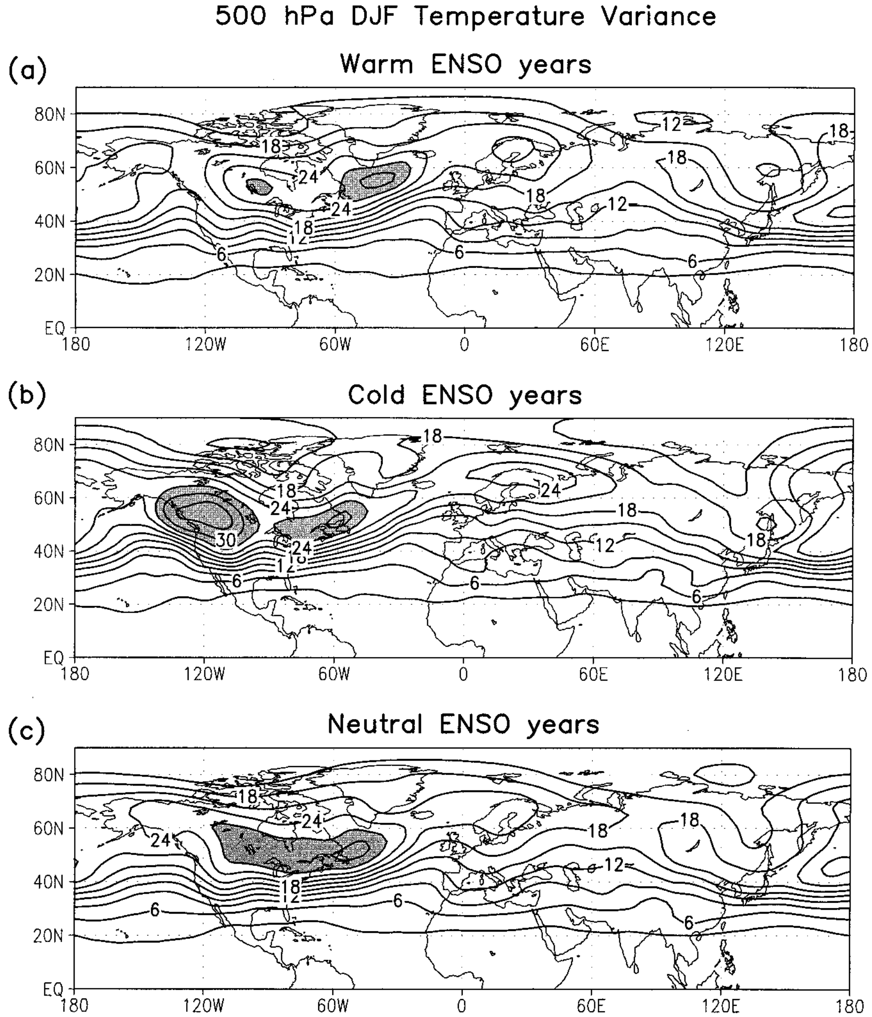

FIG. 4. The 500-hPa DJF temperature variance from the NCEP–NCAR reanalysis for (a) warm, (b) cold, and (c) neutral ENSO years during the period of Dec 1958–Nov 1996. Values every 3°C² are contoured, and values greater than 27°C² are shaded. The warm event years are 1963, 1965, 1969, 1972, 1976, 1982, 1986, 1990, 1991, 1992, and 1994, where the year corresponds to Dec in the DJF period. The cold event years are 1964, 1970, 1973, 1975, 1988, and 1995. All other years are neutral.

lation (ENSO). We, therefore, formed averages of DJF var(T) based upon warm, cold, and neutral ENSO years to determine if a portion of the interannual variance that we observed was due to the impact of ENSO upon the regional circulation (Fig. 4). The warm and cold years from 1958 to 1988 were taken from a list compiled by Kiladis and Diaz (1989) and thereafter from a compilation of warm and cold years from the National Oceanic and Atmospheric Administration (NOAA) Climate Prediction Center (see legend to Fig. 4 for a list of the warm and cold years). In comparison with the neutral years, warm years are characterized by decreased var(T) over northwestern North America, whereas cold years show an increase in var(T) over this region. These changes in 500-hPa var(T) may be a reflection of more frequent synoptic-scale cyclones in the Pacific Northwest during La Niña events (Noel and Changnon 1998). There is little indication of differences elsewhere in the globe, suggesting that the impact of ENSO upon var(T) is confined to North America.

c. The linear trend in 500-hPa temperature variance

Maps of linear trends in var(T) over the Northern Hemisphere for the 38-yr period of December 1958–November 1996 from the NCEP–NCAR dataset are presented in Fig. 5. Neglecting areas equatorward of 20°N where the trends are of negligible magnitude, we find that, in all seasons, greater than 5% of the map area is covered by statistically significant trends. Recognizing, though, that spatial correlation among neighboring points exists, we tested for the field significance of the

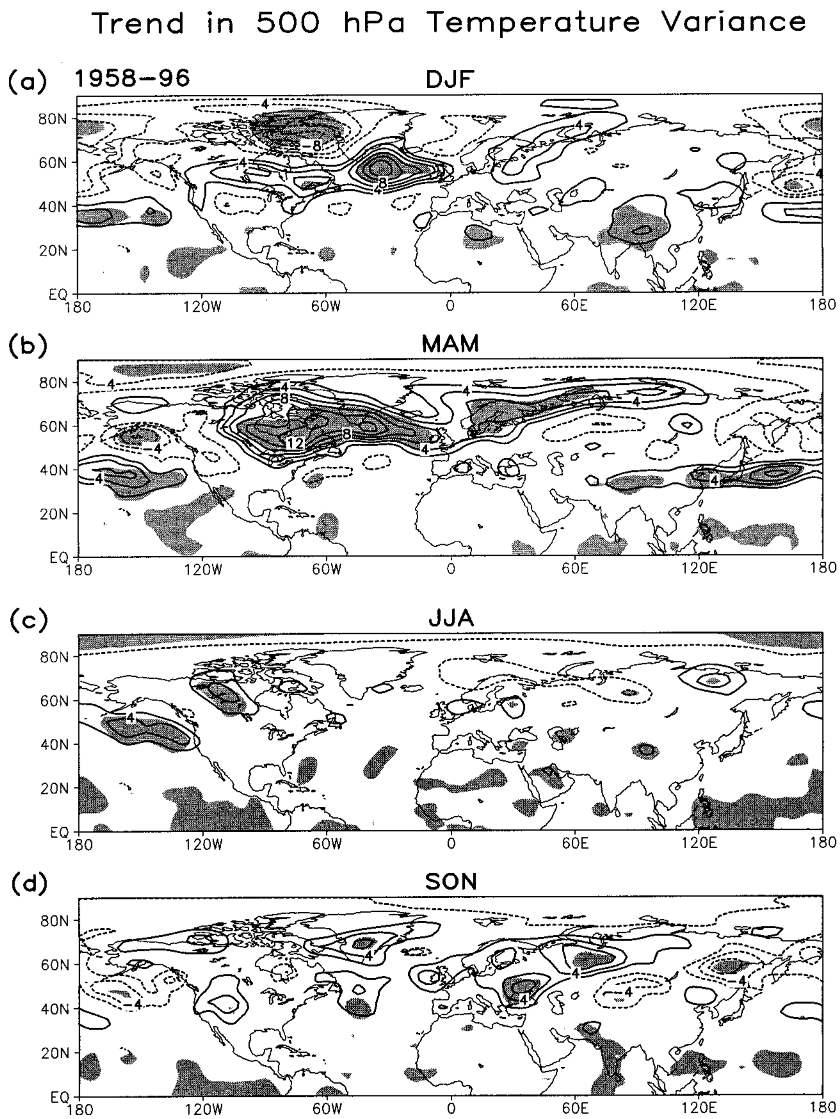

FIG. 5. The linear trend in submonthly 500-hPa temperature variance during the period of Dec 1958–Nov 1996 for (a) DJF, (b) MAM, (c) JJA, and (d) SON. Values every 2°C^2 (38 yr)$^{-1}$ are contoured; zero lines have been omitted for clarity. Solid contours represent positive values and dashed contours represent negative values. Shading indicates regions where the trends are significant at the 5% level according to a Student's *t* test based upon a Spearman rank correlation coefficient.

maps using the Monte Carlo technique of Livezey and Chen (1983). For a given season, we randomly reordered the 38 grids of var(T) 200 times and determined the putative trend at each grid point for each reshuffling. We formed maps of these gridpoint trends and calculated the percentage of map area covered by significant trends on each of the 200 maps. Comparing the observed percentage values to the resulting Monte Carlo–based distribution, we are able to reject, with 95% confidence, the hypothesis that the areas of significant trends on the DJF, MAM, and JJA maps in Fig. 5 resulted from chance.

In DJF, significant positive trends are located over the North Atlantic, southern Asia, and the central Pacific, and significant negative trends exist over the higher latitudes of North America, northwest of Alaska, and the North Pacific. In MAM, a large area of significant positive trends extends eastward from the northeastern portion of North America to northern Europe, and a second area of significant positive trends stretches across the central Pacific along 40°N from central Asia to the eastern Pacific. The positive trends in the Atlantic sector in DJF and MAM reach values of about 10°C^2 (38 yr)$^{-1}$ and, therefore, represent about 30% of the seasonal-mean values in this region (Figs. 1a,b). Significant negative trends in MAM are confined to the polar region

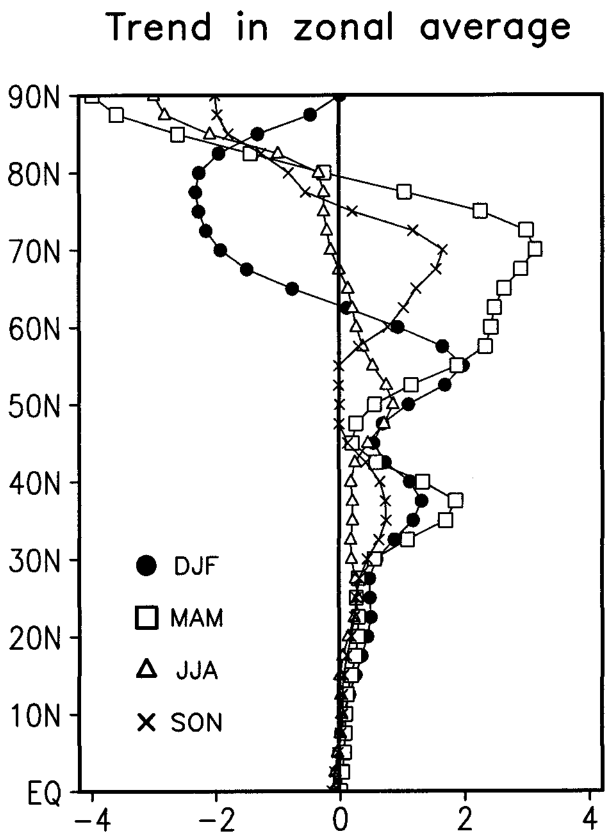

FIG. 6. The 38-yr linear trend [°C^2 (38 yr)$^{-1}$] in the zonally averaged 500-hPa Northern Hemisphere temperature variance for (a) DJF (solid circle), (b) MAM (square), (c) JJA (triangle), and (d) SON (cross).

and just south of Alaska. In JJA and SON, the trends are generally weaker than in DJF and MAM. Significant positive trends in JJA are positioned south of Alaska and over central Canada, and significant negative trends are mostly confined to the highest latitudes.

Trends in the zonally averaged var(T) in the Northern Hemisphere are shown in Fig. 6. Positive trends in var(T) generally exist in the midlatitudes; these trends are consistent with positive trends in midlatitude 500-hPa cyclone frequencies found by Key and Chan (1999). The near-polar regions are characterized by negative trends, but near 70°N a broad range of values exists, from large positive trends in MAM to large negative trends in DJF. The trends in the Tropics are generally negligible, as noted in connection with the trend maps in Fig. 5.

Overall, it appears from Fig. 6 that there has been a positive trend in var(T) at most latitudes, which implies a positive trend in area-averaged var(T) over the Northern Hemisphere. The area-averaged 500-hPa var(T) over the Northern Hemisphere for each season is shown in Fig. 7, along with the linear trend line. All seasons do exhibit positive trends in Northern Hemisphere var(T), although the trends are in all cases less than 1°C^2 (38 yr)$^{-1}$. The largest trend is in MAM, and it is the only one that is statistically significant at the 5% level in the 1958–96 period.

Although not shown here, we also examined regional trends computed from the Oort dataset for the years that it has in common with the NCEP–NCAR dataset (1958–89). Some significant areas of agreement, such as over the North Atlantic, do exist between the two datasets, but notable differences are also present, particularly over an extensive area of Asia where the Oort dataset indicates mainly negative trends for all seasons with typical values of -6°C^2 (31 yr)$^{-1}$, but the NCEP–NCAR data (see also Fig. 5) indicate a mixture of positive and negative trends of lesser absolute value. The negative trends in var(T) over Asia in the Oort data greatly impact the hemispheric trend in this dataset, as shown in Table 1a. As previously noted in our discussion of Fig. 7, over the Northern Hemisphere the trends in the NCEP–NCAR reanalysis are positive in all seasons. In the Oort data, however, the trend is negative in all seasons, and larger in magnitude than in the NCEP–NCAR reanalysis, indicating a considerable amount of disagreement between the datasets for the hemispheric average. Over the United States, on the other hand, the two datasets agree by showing mostly small positive trends (Table 1b), although these trends are not significant. The positive trends in midtropospheric var(T) over the United States are in contrast to the significant negative trends in day-to-day surface temperature variability found by Karl et al. (1995c) over the United States for 1911–92. Note, however, that the trends for the United States in Table 1b are for a different level and period than in Karl et al. (1995c).

5. Summary and concluding remarks

This investigation documents the interannual variability and secular trend in the submonthly 500-hPa temperature variance, var(T). The time-mean var(T) from a 38-yr NCEP–NCAR reanalysis dataset shows a zonally oriented maximum in the midlatitudes of both the Northern and Southern Hemispheres. The seasonal-mean values of var(T) indicate an equatorward shift of this maximum from the warm to cool season. These two observations indicate that the submonthly 500-hPa var(T) is a measure of baroclinic synoptic-scale activity associated with the midlatitude jet. In the future, we expect to apply a digital filter to our daily temperature series to determine more clearly the contribution of synoptic-scale transients to submonthly var(T).

The interannual standard deviation of the DJF 500-hPa var(T) was computed for the Northern Hemisphere to display year-to-year changes in wintertime submonthly midtroposphere temperature variance. The maximum interannual variance is over the landmasses of North America, northern Europe, and eastern Asia. The magnitude of the interannual fluctuations in the 500-hPa var(T) is about 30% of the regional DJF seasonal-mean values. A portion of the interannual variance

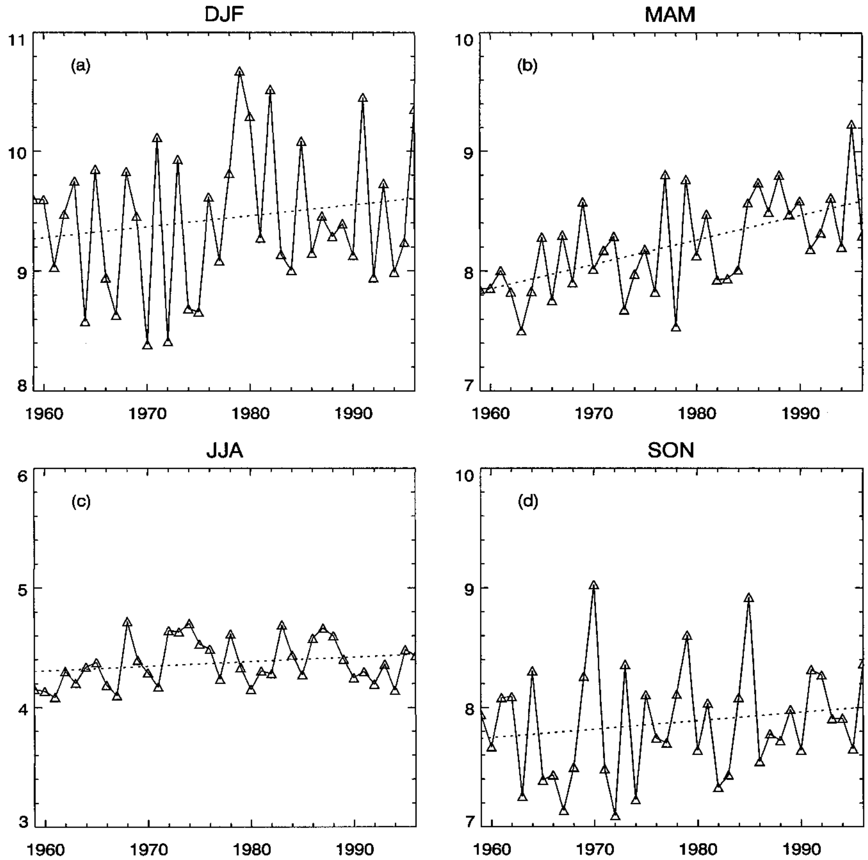

FIG. 7. Time series of 500-hPa temperature variance (°C²) area-averaged over the Northern Hemisphere for the 38-yr period of 1958–96 for (a) DJF, (b) MAM, (c) JJA, and (d) SON. The linear trend is shown by the dotted line. Note the different ranges of values on the *y* axis.

over North America may be attributable to ENSO, because there is an increase in var(T) over northwestern North America during cold events, which is consistent with an increase in storm activity over the Pacific Northwest during La Niña. Otherwise, we find little evidence that teleconnections exist among the centers of interannual variance in var(T).

TABLE 1. Trend in 500-hPa temperature variance [°C² (38-yr)$^{-1}$] area-averaged over the (a) Northern Hemisphere and (b) United States from the NCEP–NCAR and Oort datasets for the period of 1958–89. The United States region is bounded by 28°–48°N, 65°–125°W. The numbers in parentheses are for the period of 1958–96, and bold indicates trends that are significant at the 5% level.

Season	NCEP–NCAR	Oort
(a)	Northern Hemisphere	
DJF	0.3 (0.3)	**−1.7**
MAM	**0.7 (0.8)**	**−1.8**
JJA	**0.3** (0.1)	**−1.5**
SON	0.2 (0.3)	**−1.6**
(b)	United States	
DJF	0.2 (−0.1)	0.3
MAM	0.3 (0.1)	0.0
JJA	0.6 (0.2)	0.6
SON	0.2 (0.7)	−0.8

KEY: Ending date 1989 (1996).

The linear trend of the 500-hPa var(T) was computed for four seasons: DJF, MAM, JJA, and SON. The trends are largest in the middle and polar latitudes in DJF and MAM, and the trends in the Tropics are negligible in all seasons. In general, the results from the NCEP–NCAR reanalysis indicate positive trends in the 500-hPa var(T) in midlatitudes and negative trends in polar latitudes, although there is considerable seasonal variability. Over the Northern Hemisphere as a whole, there are positive trends in all seasons of less than 1°C² (38 yr)$^{-1}$, although only the trend in MAM is statistically significant for 1958–96. Regionally, the areas of greatest positive trends are positioned over northeastern North America, the northern Atlantic, northern Europe, and the central Pacific, while the largest negative trends exist over extreme northern North America and the northern Pacific.

We also compared var(T) from the NCEP–NCAR reanalysis with that from a purely radiosonde-based dataset, the so-called Oort dataset. The time-mean values of var(T) agree well for the 31-yr period when the two datasets overlap, although there is a tendency for larger values in the Oort data. These larger values are apt to be due to differences in the analysis procedure between the two datasets, such as treatment of outliers in the observations. Above northern North America and the North Atlantic, both datasets detect positive trends in var(T). It is interesting that Karl and Easterling (1999) report growing evidence for an increase in storm intensity during the past two decades over the North Atlantic. For the conterminous United States as a whole, we find no significant trends in var(T), and therefore we cannot state with confidence that there has been a change in synoptic-scale temperature variance in the midtroposphere over the United States since 1958. This null result for upper-air temperature variance is consistent with model results discussed in the introduction (Rind et al. 1989) that suggest a definitive trend in surface temperature variance over the United States need not be expected. Over Asia, the NCEP–NCAR reanalysis indicates areas of mixed positive and negative trends, but the Oort data indicate primarily negative trends over the same region. This difference is puzzling because both datasets rely on radiosonde measurements over land. Largely as a consequence of their differences over Asia, opposite results are obtained for the two datasets when the trend in area-averaged var(T) over the entire Northern Hemisphere is considered. Given these discrepancies in the hemispheric trend, it would be useful to explore this issue further with additional datasets, such as the Comprehensive Aerological Reference Data Set (Doty 1992; Eskridge et al. 1995).

Acknowledgments. We thank David Salstein for his suggestions and contributions, and Peter Nelson for providing software support. We also acknowledge Muthuvel Chelliah and Gerry Bell at NCEP for their help, and we thank the editor and anonymous reviewers for their suggestions that improved the manuscript. The research reported here has been supported with funds made available by the joint NOAA/Department of Energy Climate Change Detection and Attribution Project through Grants NA66GP0411 and NA86GP0323.

REFERENCES

Angell, J. K., 1990: Variations in global tropospheric temperature after adjustment for the El Niño influence. *Geophys. Res. Lett.,* **17,** 1093–1096.

Barnett, T. P., 1978: Estimating variability of surface air temperature in the Northern Hemisphere. *Mon. Wea. Rev.,* **106,** 1353–1367.

Barron, E. J., 1995: Forum on Global Change Modeling. Rep. USGCRP-95-01, 17 pp. [Available from Office of the U.S. Global Change Research Program, 300 D Street, SW, Suite 840, Washington, DC 20024.]

Basist, A., and M. Chelliah, 1997: Comparison of tropospheric temperature derived from the NCEP/NCAR reanalysis, NCEP operational analysis, and the microwave sounding unit. *Bull. Amer. Meteor. Soc.,* **78,** 1431–1447.

Bates, G. T., and G. A. Meehl, 1986: The effect of CO_2 concentration on the frequency of blocking in a general circulation model coupled to a simple mixed layer ocean model. *Mon. Wea. Rev.,* **114,** 687–701.

Bengtsson, L., M. Botzet, and M. Esch, 1996: Will greenhouse gas–induced warming over the next 50 years lead to higher frequency and greater intensity of hurricanes? *Tellus,* **48A,** 57–73.

Blackmon, M. L., R. A. Madden, J. M. Wallace, and D. S. Gutzler, 1979: Geographical variations in the vertical structure of geopotential height fluctuations. *J. Atmos. Sci.,* **36,** 2450–2466.

Boer, G. J., 1995: Some dynamical consequences of greenhouse gas warming. *Atmos.–Ocean,* **33,** 731–751.

——, and K. Higuchi, 1980: A study of climate variability. *Mon. Wea. Rev.,* **108,** 1326–1332.

——, and ——, 1981: Seasonal climate variability. *Atmos.–Ocean,* **19,** 90–102.

Bove, M. C., D. F. Zierden, and J. J. O'Brien, 1998: Are Gulf hurricanes getting stronger? *Bull. Amer. Meteor. Soc.,* **79,** 1327–1328.

Branscome, L. E., and W. J. Gutowski Jr., 1992: The impact of doubled CO_2 on the energetics and hydrologic processes of mid-latitude transient eddies. *Climate Dyn.,* **8,** 29–37.

Chan, J. C. L., and J. Shi, 1996: Long-term trends and interannual variability in tropical cyclone activity over the western North Pacific. *Geophys. Res. Lett.,* **23,** 2765–2767.

Christy, J. R., R. W. Spencer, and R. T. McNider, 1995: Reducing noise in the MSU daily lower-tropospheric global temperature dataset. *J. Climate,* **8,** 888–896.

Doty, S. R., 1992: The Comprehensive Aerological Reference Data Set. *Earth System Monitor,* **3,** 9–12.

Eskridge, R. E., O. A. Alduchov, I. V. Chernykh, Z. Panmao, A. C. Polansky, and S. R. Doty, 1995: A Comprehensive Aerological Reference Data Set (CARDS): Rough and systematic errors. *Bull. Amer. Meteor. Soc.,* **76,** 1759–1775.

GARP, 1975: The Physical Basis of Climate and Climate Modelling. GARP Pub. Ser. No. 16, 265 pp. [Available from the Secretariat of the WMO, Case Postale No. 5, CH-1211, Geneva 20, Switzerland.]

Gutowski, W. J., Jr., P. C. Nendick, and L. E. Branscome, 1995: Sensitivity of transient eddies to climate change in the CCC general circulation model. *Atmos.–Ocean,* **33,** 753–770.

Gutzler, D. S., R. D. Rosen, D. A. Salstein, and J. P. Peixoto, 1988: Patterns of interannual variability in the Northern Hemisphere wintertime 850 mb temperature field. *J. Climate,* **1,** 949–964.

Held, I. M., 1993: Large-scale dynamics and global warming. *Bull. Amer. Meteor. Soc.,* **74,** 228–241.

Henderson-Sellers, A., and Coauthors, 1998: Tropical cyclones and global climate change: A Post-IPCC assessment. *Bull. Amer. Meteor. Soc.,* **79,** 19–38.

Hurrell, J. W., and K. E. Trenberth, 1996: Satellite versus surface estimates of air temperature since 1979. *J. Climate,* **9,** 2222–2232.

Kalnay, E., and Coauthors, 1996: The NCEP/NCAR 40-Year Reanalysis Project. *Bull. Amer. Meteor. Soc.,* **77,** 437–471.

Karl, T. R., and R. W. Knight, 1997: The 1995 Chicago heat wave: How likely is a recurrence? *Bull. Amer. Meteor. Soc.,* **78,** 1107–1119.

——, and D. R. Easterling, 1999: Climate extremes: Selected review and future research directions. *Climatic Change,* **42,** 309–325.

——, R. W. Knight, D. R. Easterling, and R. G. Quayle, 1995a: Indices of climate change for the United States. *Bull. Amer. Meteor. Soc.,* **77,** 279–292.

——, ——, ——, and ——, 1995b: Trends in U.S. climate during the twentieth century. *Consequences,* **1,** 3–12.

——, ——, and N. Plummer, 1995c: Trends in high-frequency climate variability in the twentieth century. *Nature,* **377,** 217–220.

Katz, R. W., and B. G. Brown, 1992: Extreme events in a changing climate: Variability is more important than averages. *Climatic Change,* **21,** 289–302.

Key, J. R., and A. C. K. Chan, 1999: Multidecadal global and regional trends in 1000 mb and 500 mb cyclone frequencies. *Geophys. Res. Lett.,* **26,** 2053–2056.

Kiladis, G. N., and H. F. Diaz, 1989: Global climate anomalies associated with extremes in the Southern Oscillation. *J. Climate,* **2,** 1069–1090.

Kim, K.-Y., G. R. North, and G. C. Hegerl, 1996: Comparisons of the second-moment statistics of climate models. *J. Climate,* **9,** 2204–2221.

Kunkel, K. E., R. A. Pielke Jr., and S. A. Changnon, 1999: Temporal fluctuations in weather and climatic extremes that cause economic and human health impacts: A review. *Bull. Amer. Meteor. Soc.,* **80,** 1077–1098.

Lambert, S. J., 1995: The effect of enhanced greenhouse warming on winter cyclone frequencies and strengths. *J. Climate,* **8,** 1447–1452.

——, 1996: Intense extratropical Northern Hemisphere winter cyclone events. *J. Geophys. Res.,* **101,** 21 319–21 325.

Landsea, C. W., N. Nicholls, W. M. Gray, and L. A. Avilia, 1996: Quiet early 1990s continues trend of fewer intense Atlantic hurricanes. *Geophys. Res. Lett.,* **23,** 1697–1700.

Livezey, R. E., and W. Y. Chen, 1983: Statistical field significance and its determination by Monte Carlo techniques. *Mon. Wea. Rev.,* **111,** 46–59.

Mann, M. E., and J. Park, 1996: Joint spatiotemporal modes of surface temperature and sea level pressure variability in the Northern Hemisphere during the last century. *J. Climate,* **9,** 2137–2162.

Mantua, N. J., S. R. Hare, Y. Zhang, J. M. Wallace, and R. C. Francis, 1997: A Pacific interdecadal climate oscillation with impacts on salmon production. *Bull. Amer. Meteor. Soc.,* **78,** 1069–1079.

Nicholls, N., G. V. Gruza, J. Jouzel, T. R. Karl, L. A. Ogallo, and D. E. Parker, 1996: Observed climate variability and change. *Climate Change 1995—The Science of Climate Change,* J. J. Houghton et al., Eds., Cambridge University Press, 133–192.

Noel, J., and D. Changnon, 1998: A pilot study examining U.S. winter cyclone frequency patterns associated with three ENSO parameters. *J. Climate,* **11,** 2152–2159.

Oort, A. H., and H. Liu, 1993: Upper-air temperature trends over the globe. *J. Climate,* **6,** 292–307.

Parker, D. E., M. Gordon, D. P. N. Cullum, D. M. H. Sexton, C. K. Folland, and N. Rayner, 1997: A new global gridded radiosonde temperature data base and recent temperature trends. *Geophys. Res. Lett.,* **24,** 1499–1502.

Peixoto, J. P., and A. H. Oort, 1992: *Physics of Climate.* American Institute of Physics, 520 pp.

Prabhakara, C., R. Iacovazzi Jr., J.-M. Yoo, and G. Dalu, 1998: Global warming deduced from MSU. *Geophys. Res. Lett.,* **25,** 1927–1930.

Rind, D., R. Goldberg, and R. Ruedy, 1989: Change in climate variability in the 21st century. *Climatic Change,* **14,** 5–37.

Ross, R. J., and W. P. Elliott, 1996: Tropospheric water vapor climatology and trends over North America: 1973–93. *J. Climate,* **9,** 3561–3574.

Santer, B. D., J. J. Hnilo, T. M. L. Wigley, J. S. Boyle, C. Doutriaux, M. Fiorino, D. E. Parker, and K. E. Taylor, 1999: Uncertainties in ''observational'' estimates of temperature change in the free atmosphere. *J. Geophys. Res.,* **104,** 6305–6333.

Tarleton, L. F., and R. W. Katz, 1995: Statistical explanation for trends in extreme summer temperatures at Phoenix, Arizona. *J. Climate,* **8,** 1704–1708.

Trenberth, K. E., and J. W. Hurrell, 1994: Decadal atmosphere–ocean variations in the Pacific. *Climate Dyn.,* **9,** 303–319.

Venne, D. E., and D. G. Dartt, 1990: An examination of possible solar cycle–QBO effects in the Northern Hemisphere troposphere. *J. Climate,* **3,** 272–281.

Wagner, D., 1996: Scenarios of extreme temperature events. *Climatic Change,* **33,** 385–407.

The WASA Group, 1998: Changing waves and storms in the Northeast Atlantic? *Bull. Amer. Meteor. Soc.,* **79,** 741–760.

Wentz, F. J., and M. Schabel, 1998: Effects of orbital decay on satellite-derived lower-tropospheric temperature trends. *Nature,* **394,** 661–664.

Wilks, D. S., 1995: *Statistical Methods in the Atmospheric Sciences.* Academic Press, 467 pp.

Zhang, Y., and W.-C. Wang, 1997: Model-simulated northern winter cyclone and anticyclone activity under a greenhouse warming scenario. *J. Climate,* **10,** 1616–1634.